BMC Molecular and Cell Biology

RESEARCH

Open Access

Mutant *Fam20c* knock-in mice recapitulate both lethal and non-lethal human Raine Syndrome

Mengnan Chen[1†], Dongmei Sun[1†], Siu-Pok Yee[2†], Zhaoyang Yuan[1], Li Lin[1], Bing Cui[1], Yi Wang[3], Chao Liu[4*] and Peihong Liu[1*]

Abstract

Background Inactivation or mutations of *FAM20C* causes human Raine Syndrome, which manifests as lethal osteosclerosis bone dysplasia or non-lethal hypophosphatemia rickets. However, it is only hypophosphatemia rickets that was reported in the mice with *Fam20c* deletion or mutations. To further investigate the local and global impacts of *Fam20c* mutation, we constructed a knock-in allele carrying *Fam20c* mutation *(D446N)* found in the non-lethal Raine Syndrome. The *Fam20c*^{D446N} allele replaced the WT *Fam20c* by *3.6Kb Col1a1-Cre* to get the conditional knock-in mice, and by *Hprt-cre* to get conventional knock-in mice, respectively.

Results The radiology, serum biochemistry and immunohistochemistry indicated that all conditional and most conventional *Fam20c*^{D446N} knock-in mice displayed hypophosphatemic rickets with the increased *Fgf23* and deceased *Dmp1* expression, which survived to adulthood. However, a few conventional *Fam20c*^{D446N} knock-in mice died before weaning with the osteosclerotic X-ray radiography, though micro-CT assay displayed a reduced mineral density and increased porosity in the osteosclerotic tibia. Our results suggested that hypophosphatemia rickets was the predominant phenotype in both conditional and conventional *Fam20c* deficient mice, while the lethal osteosclerotic phenotype occasionally took place in the conventional *Fam20c* mutant mice.

Conclusion This finding also implicated that the osteosclerotic features resulting from *Fam20c* deficiency could be a semblance on the basis of rickets, which is most likely triggered by the alterations in the systems other than skeleton.

Keywords FAM20C, Raine syndrome, Osteosclerosis, Hypophosphataemic rickets, Biomineralization

†Mengnan Chen, Dongmei Sun and Sui-Pok Yee contributed equally to this work.

*Correspondence:
Chao Liu
cliu@dmu.edu.cn
Peihong Liu
xiaopei76@hrbmu.edu.cn

[1]Department of Stomatology, The First Affiliated Hospital of Harbin Medical University, Harbin, Heilongjiang 150001, China
[2]Department of Cell Biology, Health Science Center, University of Connecticut, Farmington 06030, USA
[3]Department of Prosthodontics, School of Stomatology, Dalian Medical University, Dalian 116044, China
[4]Department of Oral Pathology, School of Stomatology, Dalian Medical University, Dalian 116044, China

Background

Family with sequence similarity 20-member C (*FAM20C*) encodes the kinase of FAM20C which resides in Golgi apparatus and plays critical roles in secreted pathway [1–4]. Previous study demonstrated that FAM20C phosphorylates more than 70% of the secreted phosphoproteome by specifically recognizing and phosphorylating the S-X-E (Serine-any-Glutamate) motif [5, 9]. The wide spectrum of FAM20C substrates includes not only the extracellular matrices for skeletogenesis and biomineralization, but also soluble growth factors, adhesion molecules, etc., which is coincided to the ubiquitous *FAM20C* expression in both mineralized or non-mineralized tissues [6–8].

FAM20C deficiency in human causes Raine Syndrome [OMIM: 259775] that displays the controversial clinical manifestations, the lethal osteosclerotic bone dysplasia or the non-lethal hypophosphataemia rickets [9–13]. Through multiple genetic mouse models, hypophosphataemia rickets resulted from *Fam20c* deficiency have been well documented. Conventional inactivation or conditional abrogation of *Fam20c* in osteogenic tissues of mice reduced *Dmp1* expression, but increased the Fgf23 concentration in circulating blood, both of which were able to independently trigger hypophosphataemia rickets by decreasing serum phosphorus [14]. Further investigation indicated that Fam20c regulates the life-span of Fgf23 by phosphorylating Fgf23 on Ser^{180} [15]. Lack of the phosphorylation on Ser^{180} of Fgf23 increased the glycosylation on Thr^{178}, which blocked the cleavage of Fgf23 between Arg^{179} and Ser^{180} by Furin. Thus, *Fam20c* deficiency increases Fgf23 concentration in circulating blood by elongating its half-life, which in turn, promotes the excretion of phosphate and eventually causes hypophosphataemia rickets.

In contrast to hypophosphataemic rickets, the molecular mechanism resulting in the lethal osteosclerotic bone dysplasia in Rain Syndrome remains elusive. Previously, it is assumed that the lethal osteosclerotic bone dysplasia resulted from the enhanced kinase activity of *FAM20C* by certain point mutations. However, the *Fam20c* knock-out mice expressing the transgenic *Fam20c*^{G374R} (a mutation from the lethal osteosclerotic bone dysplasia of human Raine Syndrome) also exhibited the typical features of hypophosphataemic rickets, including the decreased bone mineral density, reduced *Dmp1* expression, increased *Fgf23* expression and serum Fgf23 concentration, though all the *Fam20c* knock-out mice expressing *Fam20c*^{G374R} transgene died in adolescence [16]. Therefore, further investigations are required to unveil the pathogenesis of lethal osteosclerotic bone dysplasia in Rain Syndrome.

In this study, we constructed Loxp-flanked *Fam20C*^{D446N} (a mutation from the non-lethal hypophosphatemca rickets of human Raine Syndrome) knock-in allele to exclude the side effects of random insertion of transgenic *Fam20c* on phenotype. By crossing the mice carrying *Fam20c*^{D446N} knock-in alleles with *Hprt-cre* and *3.6 Kb Col1a1-Cre* lines, respectively, we generated the conventional and conditional *Fam20c*^{D446N} knock-in mice which could act as the reliable tools to explore the pathogenesis of Raine Syndrome.

Materials and methods

Ethics statements

All mouse lines were maintained and expanded in the Specific Pathogenic Free System of the Institute of Genome Engineered Animal Models for Human Diseases at Dalian Medical University. All the mouse utilization and procedures in this study were approved by the Institutional Animal Care and Use Committee at Dalian Medical University with the protocol number AEE17038. All the research performance is accorded with the NIH Guide for the Care and Use of Laboratory Animals.

Constructing conditional *Fam20C*^{D446N} knock-in allele

To construct the mouse *Fam20c*^{D446N} knock-in allele, the targeting fragment spanning from exons 7 to 10 of mouse *Fam20c* was subcloned between two loxP sequences in targeting vector. An Frt flanked PKG-Neo cassette was inserted between the exon 10 and the 3' loxP. The other fragment containing the exon 7–10 sequence fused with an IRES-eGFP element was ligated downstream to the 3' loxP. The 5' homologous arm of the targeting vector was 5.4Kb long and subcloned into the vector upstream of the 5' loxP, while the 3' homologous arm was 4.1Kb long and subcloned into the vector downstream of the *IRES-eGFP* element. Finally, a negative selection MC1-HSC-TK cassette was subcloned into the downstream of the 3' homologous arm in the targeting vector. The final targeting construct was linearized with NotI and electroporated into W4 ES cells. After G418 selection, the genomic DNA was extracted from the ES clones and a 30 PCR screen was performed to screen the targeted clones. The 5' screen was performed with *Fam20c-ScrF2* as the forward primers (5'-TTTCTGTCCTAGGTAAGGGTG A AG-3') and *Lox-ScR2* as backward primer (5'-TGAAG TTCCTATTCTATAACTTCG −3') to expand the 5.4Kb fragment. The 3' screen was performed with the forward primer (*eGFP-ScF3*:5'-AACGGC CACAATTCA GCGTGTCC-3') and backward primer (*Fam20c-ScrR2*: 5'-ACAGCT TCTTGAATTGGGATAAAG-3') to produce the 4.1 Kb fragment. The 5' and 3' screening PCR products were sequenced to confirm the presence of 5' and 3' loxP sites, the exons 7–10 containing D446N point mutation and *IRES-eGFP* element. After the neo cassette was removed from the targeted ES clones by transient transfection of pCAGGS-flpEpuro vector (Addgene,

Watertown, MA, USA), two correctly targeted ES cell clones (Clone 5 A and 10 C) were selected and injected into the blastocysts from C57BL/6 mice in the Gene targeting and Transgenic Facility, University of Connecticut Health Center, Farmington, CT, USA. The male chimeras were crossbred with C57BL/6 females to produce F1 agouti offspring. The floxed alleles of F1 agouti mice (*Fam20c*$^{D446N\text{-}flox/+}$) were genotyped by PCR analyses. With forward (*LGF*: 5'-CTATCTAAGATGTAGAAGAG GTG-3') and backward primers (*FrtR*: 5'-CTCACAGTA ATCAGGGTCGAC-3'), the WT allele produced 432 bp segment, and the *Fam20c*$^{D446N\text{-}flox}$ allele gave a 527 bp product.

Generating conditional and conventional *Fam20c*^{D446N} knock-in mice

To generate the conditional *Fam20c* knock-in mice, the *Fam20c*$^{D446N\text{-}flox/+}$ mice were first crossbred with *3.6 Kb Col1a1-Cre* transgenic mice to gave rise to *3.6 Kb Col1a1-Cre; Fam20c*$^{D446N\text{-}flox/+}$ mice, which were mated with the *Fam20c*$^{D446N\text{-}flox/+}$ mice to get the *3.6 Kb Col1a1-Cre; Fam20c*$^{D446N\text{-}flox/D446N\text{-}flox}$ mice (referred as the conditional *Fam20c*^{D446N} knock-in mice). When the *Fam20c*$^{D446N\text{-}flox/+}$ male mice were crossbred with the *Hprt-cre* female mice (Stock NO. 004302, Jackson Laboratory), the loxP flanked sequence in the conditional *Fam20c*$^{D446N\text{-}flox}$ allele would be eliminated by Cre in the fertilized eggs or blastocysts. Thus, the conditional *Fam20c*$^{D446N\text{-}flox}$ allele would be transformed into the conventional *Fam20c*$^{D446N\text{-}KI}$ allele. We mated the *Fam20c*$^{D446N\text{-}KI}$ males with the *Fam20c*$^{D446N\text{-}KI}$ females to get *Fam20c*$^{D446N\text{-}KI/D446N\text{-}KI}$ mice (referred as the conventional *Fam20c*^{D446N} knock-in mice). The gentyping PCT with the primers of *LGF* and *FrtR* produced a 374 bp fragment for the conventional *Fam20c*^{D446N} knock-in allele, which distinguished from the 527 bp fragment of the conditional *Fam20c*^{D446N} knock-in allele.

Plain X-ray and micro-CT examination

The X-ray radiography was performed by the inspector of Faxitron MX-20DC12 (Faxitron Bioptics, Tucson, Arizona, USA). The micro-CT scanning was conducted by the SCANCO Medical μCT system with a medium resolution of 7.0 mm slice increment, and the scanning data were analyzed and reconstructed by NRecon v1.6 and CTAn v1.13.8.1 software. The male WT and conditional or conventional *Fam20c*^{D446N} knock-in mice from a litter were euthanized by carbon dioxide (followed by cervical dislocation), and then, dissected to get ribs, femurs and tibia (including the knee) for X-ray radiography. For the conventional *Fam20c*^{D446N} knock-in mice die before weaning, we compared them to their littermates with same gender.

Histology and immunohistochemistry

The male P4W WT and conditional or conventional *Fam20c*^{D446N} knock-in mice from a litter mice were euthanized and dissected for the femurs. The femurs were fixed in 4% PFA overnight, separated from soft tissues, and decalcified in 15% trypsin- ethylenediaminetetraacetic acid (EDTA) for 2 weeks. The decalcified femurs were dehydrated in gradient alcohols and embedded in paraffin for the 10 μm thick slices. Masson staining for the slices was described previously. Immunohistochemical staining was performed as previously described with the antibodies against Fam20c, Fgf23 and Dmp1 [7, 17, 18]. ABC kit and the DAB kit (Vector Laboratories, Burlingame, CA) were applied to color development with the methyl green counter-staining according to the manufacturer's instructions. The negative controls of immunohistochemistry were conducted by above procedures without primary antibodies.

Serum biochemistry

The sera of male P4W WT and conditional or conventional *Fam20c*^{D446N} knock-in mice were collected as previous described [14]. Fgf23 concentration were measured with a full-length FGF23 ELISA kit (Kainos Laboratories, Tokyo, Japan), phosphorus concentration with a kit using the phosphomolybdate ascorbic acid method (Stanbio Laboratory, Boerne, TX, USA), and calcium concentration with a colorimetric calcium kit (Stanbio Laboratory, Boerne, TX, USA). All the concentrations of Fgf23, phosphorus and calcium were quantified by a SPECTRA max 250 microplate spectrophotometer (Molecular Device Corporation, Sunnyvale, California, USA).

Statistical analysis

Statistical analysis were performed using a Student t test with SPSS 21.0 software, and stated as the Mean ± SD (standard derivation). *P* value less than 0.05 was regarded as the significant difference between two individual groups. To eliminate the discrepancy between genders, only the the body weights of the male WT and conditional or conventional *Fam20c*^{D446N} knock-in mice were collected for statistical assay.

Results

Generation of conditional and conventional *Fam20c*^{D446N} knock-in mice

To generate the conditional mouse *Fam20c*^{D446N} knock-in allele, we converted the gat encoding the 446 Aspartate (D) at the Fam20c amino acid sequence into aat encoding Asparagine (N; Fig. 1A). The targeting vector contained the full length DNA from the exons 7 to 10 with the floxing loxP sites, which was followed by the cDNA from exon 7 to 10 carrying the mutation of *Fam20c*^{D446N} (*Fam20c*$^{D446N\text{-}flox}$ allele; Fig. 1B). Once gene

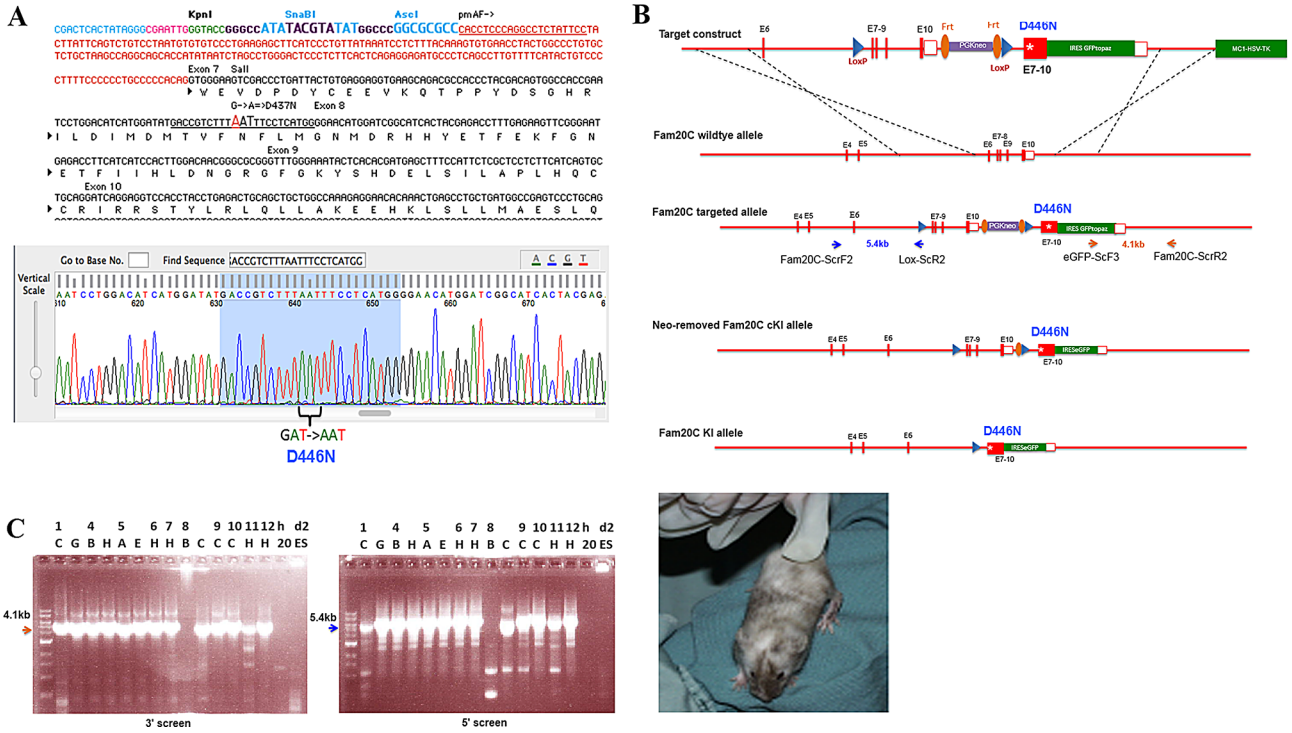

Fig. 1 Generating conditional and conventional *Fam20c*^{D446N} knock-in mice by gene targeting. (**A**) Sequencing of the targeting vector showed that the gat encoding Aspartate (D) was mutated into aat encoding Asparagine (N). (**B**) In the targeting construct, the full DNA from exon 7 to 10 and a PGK-neo cassette flanked by Frt sites (orange ovals) were flanked by loxp sites (blue triangles). A cDNA of exon 7–10 carrying the D446N mutation was fused with a *IRES-EGFP* reporter cassette and followed the loxp flanked sequence. A MC1-HSV-TK cassette was downstream to the 3'-homologous arm (target construct). The PGK-neo cassette was removed from the targeted allele after correct targeting (Neo-removed *Fam20c cKI* allele). To ensure the correct targeting, a 5.4Kb segment at 5' arm and a 4.1Kb segment at 3' arm of the target construct were tested through PCR with the primers *eGFP-ScF3* and *Fam20c-ScrR2*, and the primers *Fam20c-ScrF2* and *Lox-ScR2*, respectively (*Fam20c* targeted allele). When the loxp-flanking exon 7–10 was removed by Cre, the *Fam20c KI* allele was formed by recombining the exon 1–7 with the cDNA of exon 7–10 carrying the mutation of D446N. (**C**) PCR screening for targeted ES clones showed the correct targeting took place in 13 ES clones. Two correctly targeted ES clones (5 A and 10 C) were selected for injection and both got germline transmission

targeting was accomplished, only the full length *Fam20c* DNA was transcribed into the normal *Fam20c* mRNA, while the inserted *Fam20c* cDNA carrying point mutation would not be expressed. In the presence of Cre, the full length DNA from the exons 7 to 10 floxed by loxps was removed to form the recombined *Fam20c* knock-in allele, which was constituted by the full length DNA from exon 1 to 6, and the cDNA from 7 to 10 containing the mutation of D446N (*Fam20c*$^{D446N\text{-}KI}$ allele; Fig. 1B). The correct targeting events in ES clones were confirmed by PCR screening with the primers *eGFP-ScF3* and *Fam20c-ScrR2* for a 4.1Kb segment at 3' arm, and the primers *Fam20c-ScrF2* and *Lox-ScR2* for a 5.4Kb segment at 5' arm (Fig. 1B, C). Two correctly targeted ES cell clones were chosen for injection, and both gave chimera through germline transmission (Fig. 1C). Then, the male chimeric mouse was chosen to give agouti F1 mice which were used to generate conditional and conventional *Fam20c*^{D446N} knock-in mice as described in Materials and methods.

Rickets/osteomalacia in the conditional and conventional *Fam20c*^{D446N} knock-in mice

Compared to their WT littermates, both the conditional and conventional *Fam20c*^{D446N} knock-in mice showed obvious retardation in growth at P2W, which was still remarkable at P4W (Fig. 2A). Statistical assay of the body weights at P4W verified the discrepancy between WT, and the conditional and conventional *Fam20c*^{D446N} knock-in mice, and further indicated that there was no significant difference in body weight between the conditional and conventional *Fam20c*^{D446N} knock-in mice (Fig. 2B). As shown in plain X-ray images, both the conditional and conventional *Fam20c*^{D446N} knock-in mice exhibited a rickets/osteomamalcia characteristics in the skeleton at P4W, including not only the shorter length of femur and tibia, but also the widened growth plates and thinner tibia cortex (Fig. 2C). To P8W, the conditional and conventional *Fam20c*^{D446N} knock-in mice still showed the fainter reflection in both cortical and spongy bone of the shorted femur and tibia, though the widened growth plates were not so noticeable as those at

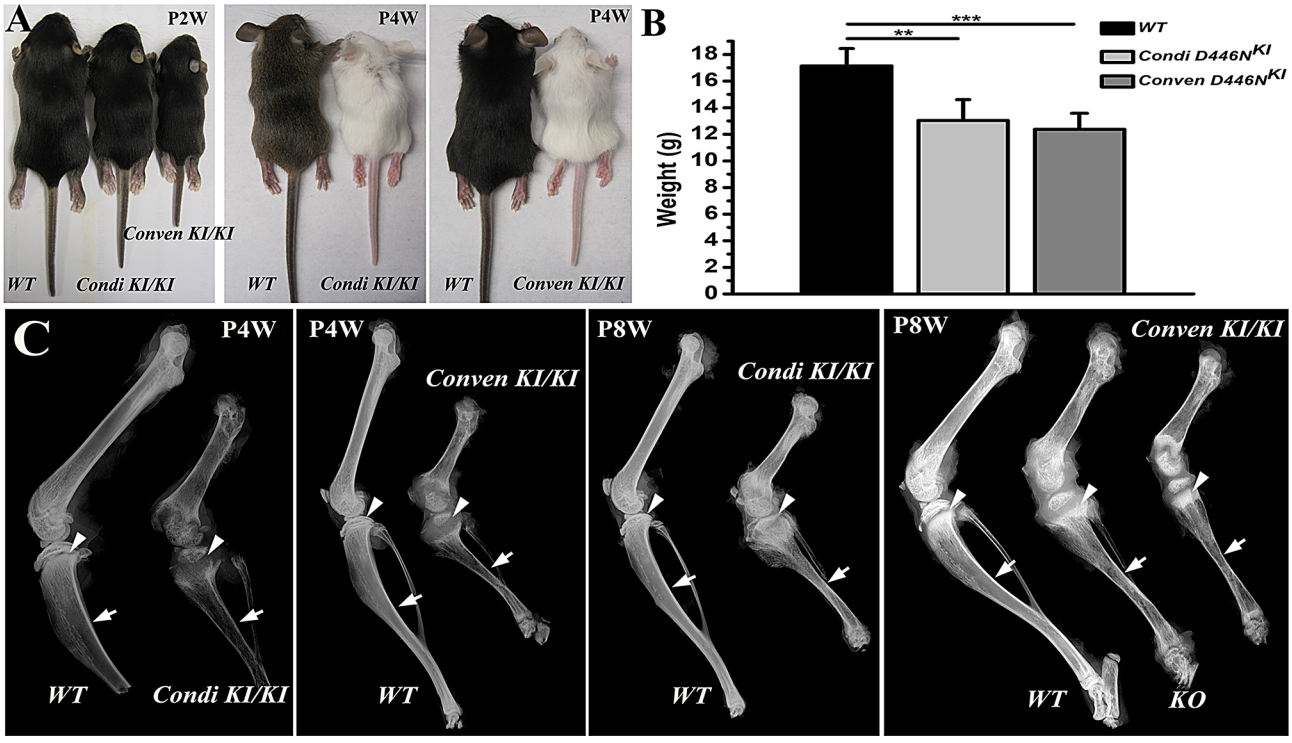

Fig. 2 The skeletal characteristics of the conditional and conventional *Fam20c*^{D446N} knock-in mice. (**A**) The gross views of the P2W WT, conditional and conventional *Fam20c*^{D446N} knock-in mice (left) and the P4W WT, conditional and conventional *Fam20c*^{D446N} knock-in mice (middle and right). (**B**) The statistical analysis on the body weights of P4W WT (17.14 ± 1.30 g), conditional (13.04 ± 1.57 g) and conventional *Fam20c*^{D446N} knock-in (12.38 ± 1.20 g) mice. (**$p < 0.01$,***$p < 0.001$). (**C**) Comparison of the plain X-ray examination on the femurs between P4W WT and conditional *Fam20c*^{D446N} knock-in mice (most left); between P4W WT and conventional *Fam20c*^{D446N} knock-in mice (the second image from left), between P8W WT and conditional *Fam20c*^{D446N} knock-in mice (the second image from right), and among P8W WT, conditional *Fam20c* knock-out (KO) and conventional *Fam20c*^{D446N} knock-in mice (most right). (Arrowheads delineated growth plates and arrows pointed to tibia cortex)

P4W. Such rickets/osteomamalcia features in the conditional and conventional *Fam20c*^{D446N} knock-in mice were similar to the *3.6 Kb Col1a1-cre; Fam20c*$^{f/f}$ mice (KO) (Fig. 2C).

Both the conditional and conventional *Fam20c*^{D446N} knock-in mice suffered from hypophosphatemic rickets

Histological analysis with Masson staining confirmed the rickets/osteomamalcia characteristics in the P4W conditional and conventional *Fam20c*^{D446N} knock-in mice. Although the gross views seemed no discrepancy (Fig. 3A-C), the growth plates in the femoral heads of the conditional and conventional *Fam20c*^{D446N} knock-in mice displayed the less proliferating chondrogenic cells and the enlongated columns of hypertrophyic chondrocytes compared to the WT controls (Fig. 3A'-C'). Consistently, the cortex in the femoral diaphysis of the conditional *Fam20c*^{D446N} knock-in mice was more porous than WT counterparts (Fig. 3A", B"). More evidently, the cortex in the conventional *Fam20c*^{D446N} knock-in femoral diaphysis was much more porous even compared to the counterpart in the conditional *Fam20c*^{D446N} knock-in mice (Fig. 3B", C").

To further explore the rickets/osteomamalcia phenotype, we performed the serum biochemistrical assays of the P4W conditional and conventional *Fam20c*^{D446N} knock-in mice. There were greatly elevated Fgf23 concentration, as well as reduced serum phosphorus and relative normal calcium concentrations in both the conditional and conventional *Fam20c*^{D446N} knock-in mice (Table 1). Worthy of notice, the serum Fgf23 concentrations in the conditional and conventional *Fam20c*^{D446N} knock-in mice were significantly higher than not only the WT mice, but also the KO mice (Table 1).

Immunohistochemical staining was preformed to verify the construction of knock-in mice and the consequence of serum biochemistry. The immuno-staining of Fam20c showed no difference among the tibiae of P4W WT, conditional and conventional *Fam20c*^{D446N} knock-in mice (Fig. 3D, D', D"). Consistent with the consequence of serum biochemistry, the Fgf23 staining in the conditional and conventional *Fam20c*^{D446N} knock-in tibiae was obvious higher than that in WT tibia (Fig. 3E, E', E"). In contrast, the conventional *Fam20c*^{D446N} knock-in tibia was almost devoid of Dmp1 staining (Fig. 3F"), while the Dmp1 staining in the conditional *Fam20c*^{D446N} knock-in tibia was much fainter than that in WT

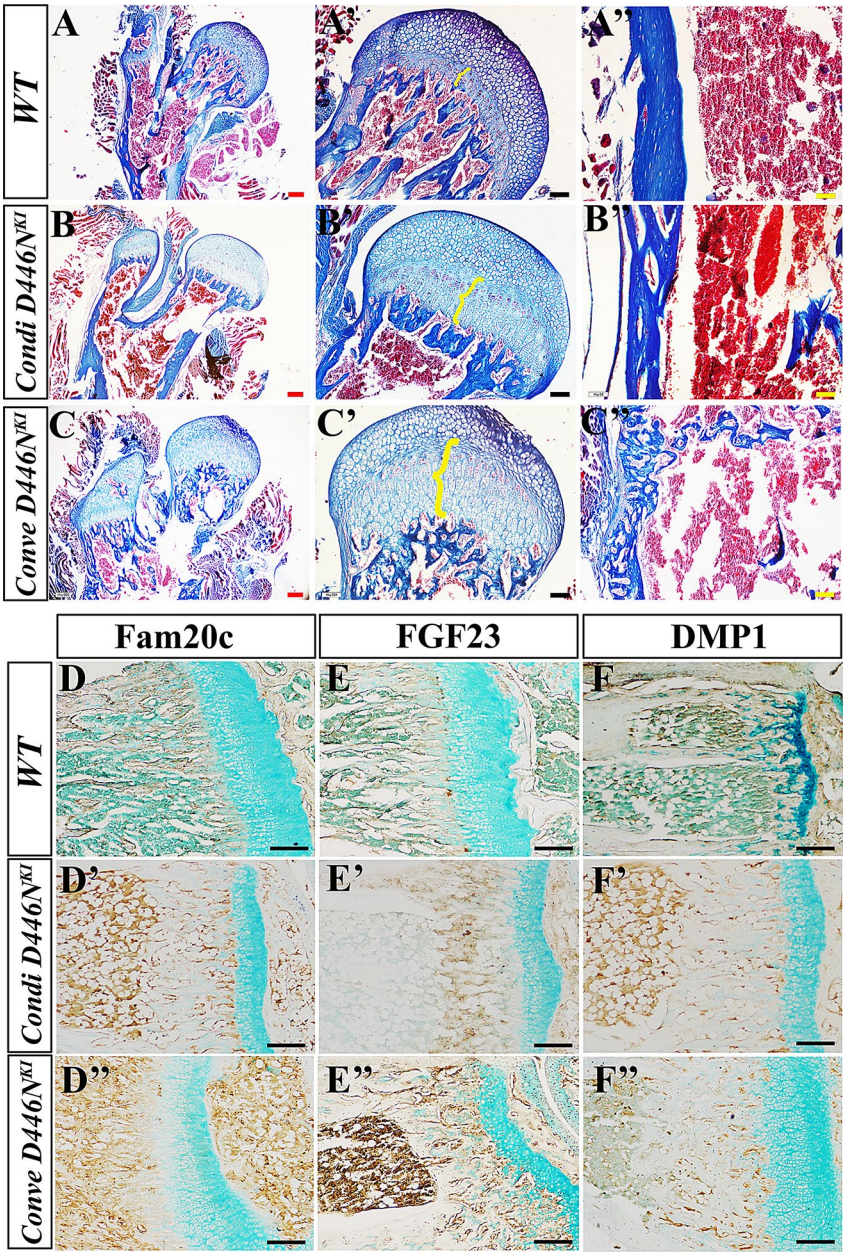

Fig. 3 The skeletal characteristics of the conditional and conventional *Fam20c*^{D446N} knock-in mice. (**A**, **A'**, **A''**) Masson staining of the P4W WT femoral metaphysis (**A**), femur heads (**A'**) and femoral cortex (**A''**). (**B**, **B'**, **B''**) Masson staining of the P4W conditional *Fam20c*^{D446N} knock-in femoral metaphysis (**B**), femur heads (**B'**) and cortex (**B''**). (**C**, **C'**, **C''**) Masson staining of the P4W conventional *Fam20c*^{D446N} knock-in femoral metaphysis (**C**), femur heads (**C'**) and cortex (**C''**). (**D**, **D'**, **D''**) Immunohistochemical staining with antibody against Fam20C in the tibiae of the P4W WT (**D**), conditional (**D'**) and conventional *Fam20c*^{D446N} knock-in mice (**D''**). (**E**, **E'**, **E''**) Immunohistochemical staining with antibody against Fgf23 in the tibiae of the P4W WT (**E**), conditional (**E'**) and conventional *Fam20c*^{D446N} knock-in mice (**E''**). (**F**, **F'**, **F''**) Immunohistochemical staining with antibody against DMP1 in the tibiae of the P4W WT (**F**), conditional (**F'**) and conventional *Fam20c*^{D446N} knock-in mice (**F''**). (The yellow parentheses indicated the width of growth plates in femurs; Scale bar is 200 μm)

controls (Fig. 3F, F'). Supplementary material 1 showed the negative controls of WT, conditional and conventional *Fam20c*^{D446N} knock-in long bones, in which only secondary antibody and color reagent were applied for color development without the primary antibodies. All of these data indicated that both the conditional and conventional *Fam20c*^{D446N} knock-in mice suffered from hypophosphatemic rickets.

A few conventional *Fam20c*^{D446N} knock-in mice died before weaning showed osteosclertic features

Although all the conditional and most conventional *Fam20c*^{D446N} knock-in mice could survive to adult and

Table 1 Serum concentration of Fgf23, pi and calcium in WT, KO, conditional and conventional *Fam20c*^{D446N} knock-in mice

Fgf23 (pg/ml)	WT	KO	Conditional D446N-KI/KI	Conventional D446N-KI/KI
Mean	354.229	2064.840	9906.574	19338.826
SD	252.613	1693.729	8875.662	10944.253
P values		0.00224 (to WT)	0.00996 (to KO)	0.00485 (to KO)
Pi (mg/dl)	**WT**	**KO**	**Conditional D446N-KI/KI**	**Conventional D446N-KI/KI**
Mean	13.826	6.834	7.890	5.56
SD	3.618	1.175	1.933	2.63
P values		0.00133 (WT)	0.301 (to KO)	0.0911 (to KO)
Calcium (mg/dl)	**WT**	**KO**	**Conditional D446N-KI/KI**	**Conventional D446N-KI/KI**
Mean	14.592	13.920	12.078	13.02
SD	2.172	2.825	1.537	2.98
P values		0.906 (to WT)	0.203 (to KO)	0.761 (to KO)

suffered from the non-lethal hypophosphatemic rickets, we indeed found several conventional *Fam20c*^{D446N} knock-in mice (less than 5% of the conventional *Fam20c*^{D446N} knock-in pups) died before weaning (P1-3 W). These died mice also exhibited growth retardation (Fig. 4A), and plain X-ray examination showed the higher reflection in the cranial base (Fig. 4B), ribs (Fig. 4C) and femurs (Fig. 4D) compared to the WT counterparts. Micro-CT 3D reconstruction showed the much more porous cortex, and the less but thickened trabecula in the osteosclerotic conventional *Fam20c*^{D446N} knock-in pups, even compared with the conditional and rickets/osteomalacia conventional *Fam20c*^{D446N} knock-in pups (Fig. 4E). Moreover, the bone mineral density of the osteosclerotic conventional *Fam20c*^{D446N} knock-in pup was even lower than that in both conditional and rickets/osteomalacia conventional *Fam20c*^{D446N} knock-in mice (Table 2). Histological assay indicated that although thicker than that of WT, conditional and the survived conventional *Fam20c*^{D446N} knock-in pups, the tibia cortex of the lethal osteosclerotic conventional *Fam20c*^{D446N} knock-in pup was much more porous (Fig. 4F), implicating the osteosclerotic features most likely a semblance in radiography. Thus, the increased X-ray reflection, especially in the ribs and femurs of conventional *Fam20c*^{D446N} knock-in mice seemed result from the more extensive deposition of mineral fibres, as apposed of the increased bone mineral density.

Discussion

Although characterized by a broader spectrum of disorders [13, 19], the key manifestations of Raine Syndrome was the skeletal defects: the sclerotic bone dysplasia or hypophosphatemia rickets [10, 20]. As the causative gene of Raine Syndrome, how the deficiency of *FAM20C* resulted in the heterogeneous, even the controversial clinical manifestations in skeleton, attracted the interests of researchers. Initially, the heterogeneous skeletal defects were speculated to result from the altered kinase activity of the *FAM20C* mutants because the lethal cases of Raine Syndrome contributed more point mutations in the conserved C-terminal kinase domain (CCD), while most point mutations in the non-lethal cases resided out of the CCD [2, 21]. However, the ex vivo study indicated that the kinase activity of the *FAM20C* mutants in both the lethal and non-lethal Raine subjects was reduced compared to WT *FAM20C*, and deletion or splicing mutations of *FAM20C* were detected in both the lethal and non-lethal cases of Raine Syndrome [9, 21]. Thus, the controversial skeletal manifestations in Raine Syndrome seems not determined by certain *FAM20C* mutations.

In our latest study, we constructed the *3.6 Kb Col1a1-cre; Fam20c*$^{f/f}$; *Fam20c*$^{G374R\text{-}Tg}$ and *3.6 Kb Col1a1-cre; Fam20c*$^{f/f}$; *Fam20c*$^{D446N\text{-}Tg}$ mice to mimic the mutations from lethal and non-lethal Raine Syndrome cases, respectively [16]. The increased porosity in cortex, the decreased trabecular amounts, the elevated serum Fgf23 and reduced phosphorus suggested that both mutant mice also underwent hypophosphatemia rickets as *3.6 Kb Col1a1-cre; Fam20c*$^{f/f}$ mice did. Furthermore, the mutant *Fam20c* from lethal and non-lethal Raine Syndrome showed no discrepancy in elevating *Fgf23* expression in both the in vivo and ex vivo conditions. These results indicated that the mutant *Fam20c* from both the lethal and non-lethal cases primarily led to the hypophosphatemia rickets/osteomalacia, instead of osteosclerosis [16].

In our present study, we generated the conditional knock-in allele of mutant Fam20c to prevent the side effects of random insertion of transgene. Taking the advantage of the conditional knock-in allele, we generated the conventional knock-in mice by *Hprt-cre* to mimic human Raine Syndrome, and the conditional knock-in mice by *3.6Kb Col1a1-cre* to explore the role of *Fam20c* in bone development and mineralization. It was found that hypophosphatemia rickets/osteomalacia was the predominant phenotype of the conditional and conventional *Fam20c*^{D446N} knock-in mice, which is consistent with the consequence from the transgenic *Fam20c* mutant mice. Unexpectedly, a few conventional *Fam20c*^{D446N} knock-in mice exhibited the osteosclerotic features. Clinically, the co-existence of osteomalacia and osteosclerotic manifestation was found not only in the subject of non-lethal Raine Syndrome [22], but also in the cases of X-linked and autosomal recessive hypophosphatemic rickets [23–25], in which most of these osteosclerosis were identified by X-ray radiography and lacked histological and quantitative evidence. However,

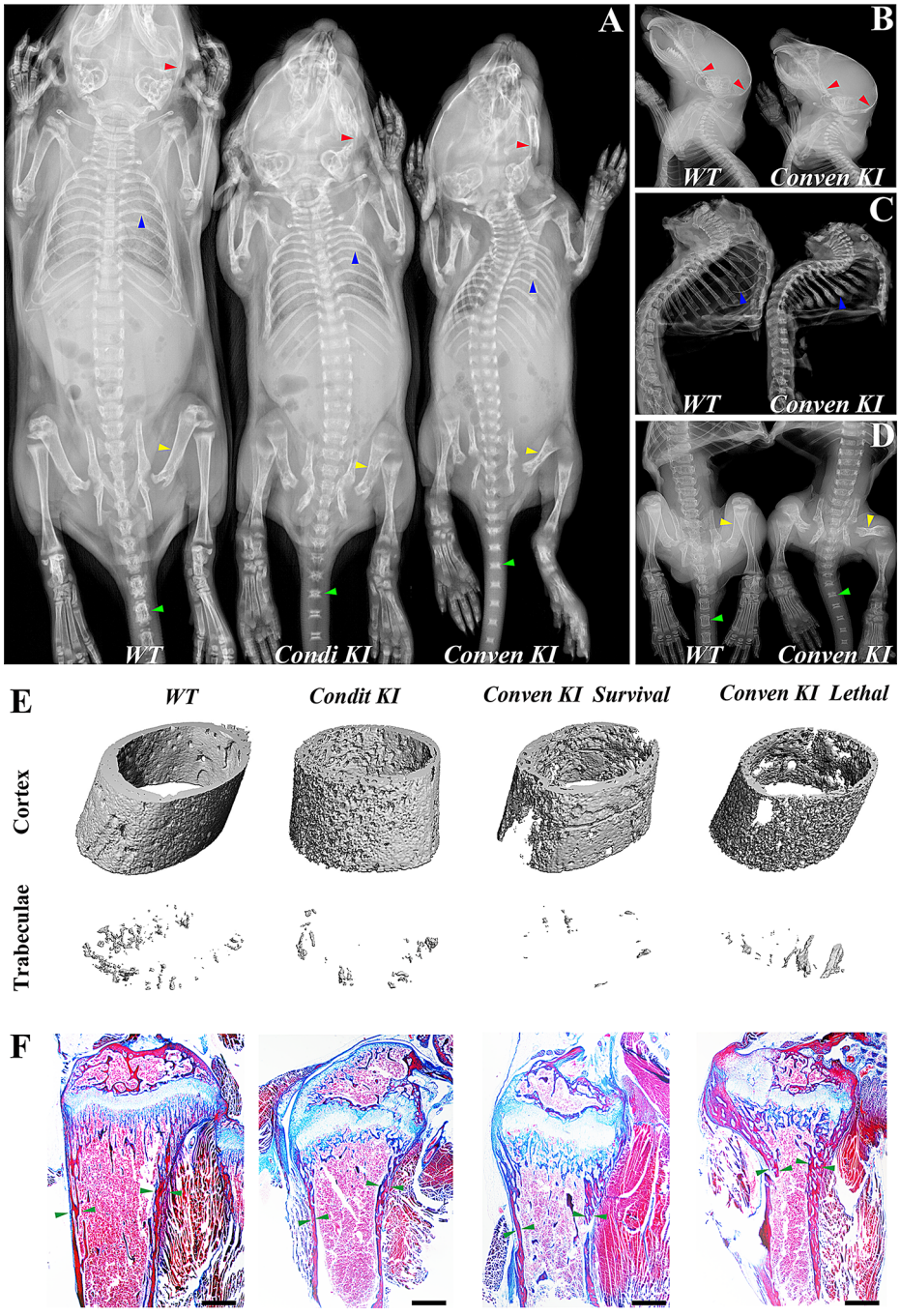

Fig. 4 The plain X-ray features of the conventional *Fam20c*^{D446N} knock-in mice died before weaning. (**A**) The plain X-ray images of the P18d WT, conditional *Fam20c*^{D446N} knock-in mice and the died conventional *Fam20c*^{D446N} knock-in mice. (**B**-**D**) There were occasional death (less than 5%) from P1W to weaning in all conventional *Fam20c*^{D446N} knock-in mice. The increased X-ray reflection was detected in the cranial bases (**B**), ribs (**C**) and femurs (**D**) of the occasionally died conventional *Fam20c*^{D446N} knock-in mice. (Red arrowheads pointed to cranial bases, yellow arrowheads to ribs, blue arrowheads to cortex in tibiae and green arrowheads to tail vertebrates) (**E**) The reconstructed cortex and trabeculae in tibiae from P24d WT, conditional *Fam20c*^{D446N} knock-in mice, as well as the survived and the died conventional *Fam20c*^{D446N} knock-in mice. (**F**) The masson staining of the tibiae from P24d WT, conditional *Fam20c*^{D446N} knock-in mice, as well as the survived and the died conventional *Fam20c*^{D446N} knock-in mice. (Green arrowheads pointed to the cortex in tibiae; Scale bar is 200 μm)

Table 2 Quantatative micro-CT analyses of the tibia from P3w WT, conditional, osteosclerotic and rickets/osteomalacia conventional *Fam20c*^{D446N} knock-in mice

Variables	WT	Conditional	Rickets Conventional	Osteosclerotic Conventional
BV/TV	~0.633	~0.394	~0.410	~0.299
Apparet density (mg/cm^3)	763.419	472.922	504.357	422.432
Material density (mg/cm^3)	884.880	807.621	836.788	785.557

the micro-CT assay indicated a reduced bone mineral density and severer porosity in the long bone of the osteosclerotic conventional *Fam20c*^{D446N} knock-in pup, supporting the assumption that *FAM20C* deficiency primarily causes hypophosphatemia rickets/osteomalacia. Moreover, our finding implicated that the osteosclerotic feature was most likely a semblance resulting from the extended deposition of mineral fibers, as apposed of a real osteosclerosis.

Because of the limited case of osteosclerotic conventional *Fam20c*^{D446N} knock-in mice, we could not exclude the osteosclerosis in Raine Syndrome. Recently, by transfecting a series of *FAM20C* mutants reported in lethal cases of Rain syndrome into human osteosarcoma cell lines, Koike et al. reported that the mutant *FAM20C* was incapable of interacting with chondroitin 4-O-sulfotransferase-1, which reduced the ratio of 4-sulfation/6-sulfation of chondroitin, and in turn, increased the amounts of mineral nodules. They further found that the balance between 4-sulfation and 6-sulfation of chondroitin played a critical role in maintaining bone mineral density, and 6-sulfation was able to enhance osteogenic differentiation ex vivo and biomineralization in vivo [26]. Since neither WT nor mutant *FAM20C* impacted the 4-sulfation/6-sulfation of chondroitin directly, how FAM20C regulates the biomineralization remains to be elucidated. We speculate that the metabolism and/or endo/paracrine altered by *FAM20C* deficiency most likely trigger osteosclerotic features, because of the ubiquitous expression of *FAM20C* and a series of substrates including endo/paracrine factors [15, 27]. Furthermore, we speculate that on the basis of hypophosphatemia rickets/osteomalacia, the various metabolic and/or endo/paracrine factors, combined with more complicated environmental influence, results in osteosclerotic dysplasia in lethal Raine Syndrome. The recent case of Rained Syndrome reported the gradually decreased osteosclerosis, subperiosteal osteoid formation and the emerging bone-in-a-bone appearance in medullary space in a subject with the increasing age supported the speculation [28].

Therefore, in our further exploration, we will accumulate more cases of the osteosclerotic conventional *Fam20c*^{D446N} knock-in mice to address the osteosclerotic characteristics. Additionally, we will examine the ratio of 4-sulfation/6-sulfation of chondroitin, as well as the activities of chondroitin 4-O-sulfotransferase-1 and chondroitin 6-O- sulfotransferase-1, in the conventional *Fam20c*^{D446N} knock-in mice with the lethal osteosclerotic features, to verify the novel mechanism of *FAM20C/Fam20c* in biomineralization.

Conclusion

We reported the non-lethal hypophosphatemia rickets/osteomalacia as the predominant phenotype of the conditional and conventional *Fam20c*^{D446N} knock-in mice, confirming our previous conclusion. We also found a few lethal ostelsclertotic cases in the conventional *Fam20c*^{D446N} knock-in mice, which recapitulated the lethal osteosclerotic bone dysplasia of human Raine Syndrome. However, the long bone of the lethal ostelsclerotic conventional *Fam20c*^{D446N} knock-in mice was in lower bone mineral density and more porous, implicating that the osteosclerotic features in Raine Syndrome most likely a semblance of extended mineral deposition, instead of a real osteosclerosis.

Supplementary Information

The online version contains supplementary material available at https://doi.org/10.1186/s12860-024-00526-4.

Supplementary Material 1

Acknowledgements

We sincerely thank Dr. Jianjun Hao in Division of Orthodontics, Department of Craniofacial Sciences, School of Dental Medicine, University of Connecticut, Farmington, USA for his instruction and efforts in generating the mouse carrying *Fam20c*^{D446N} knock-in allele.

Author contributions

C.L. and P.L.: conception, design of the research and writing of the manuscript; S.Y.: generation of the mouse carrying *Fam20c*^{D446N} knock-in allele; M.C. and D.S.: acquisition of histological data, analysis and interpretation of the data, edition of figures and tables; Z.Y.: acquisition of serm biochemistry; L.L.: X-ray plain film and micro-CT scanning; B.C.: Statistical assay; Y.W: maintaining, expanding and identifying the *Fam20c*^{D446N} knock-in mice. All authors have read and approved the final version of the manuscript.

Funding

This research was funded by the Natural Science Foundation of Heilongjiang Province (grant no. H2017030), the Fund of Harbin Science and Technology Bureau (grant no. 2022ZCZJNS055) and the Fund of the First Affiliated Hospital of Harbin Medical University (grant no. 2016B020).

Data availability

Data is provided within the manuscript or supplementary information files. All the data and materials of this study are available from the corresponding authors upon reasonable request.

Declarations

Ethics approval and consent to participate

All the experiment in this study were conducted in accordance to the guideline and regulation in the animal study protocol approved by the Ethics Committee of Dalian Medical University (Protocol number: AEE17038).

Consent for publication

Not applicable.

Competing interests

The authors declare no competing interests.

Received: 1 September 2024 / Accepted: 19 December 2024
Published online: 02 January 2025

References

1. Hao J, Narayanan K, Muni T, Ramachandran A, George A. Dentin matrix protein 4, a novel secretory calcium-binding protein that modulates odontoblast differentiation. J Biol Chem. 2007;282:15357–65. https://doi.org/10.1074/jbc.M701547200.
2. Tagliabracci VS, Engel JL, Wen J, Wiley SE, Worby CA, Kinch LN, et al. Secreted kinase phosphorylates extracellular proteins that regulate biomineralization. Science. 2012;336:1150–3. https://doi.org/10.1126/science.
3. Tagliabracci VS, Pinna LA, Dixon JE. Secreted protein kinases. Trends Biochem Sci. 2013;38:121–30. https://doi.org/10.1016/j.tibs.2012.11.008.
4. Ishikawa HO, Xu A, Ogura E, Manning G, Irvine KD. The Raine syndrome protein FAM20C is a golgi kinase that phosphorylates bio-mineralization proteins. PLoS ONE. 2012;7:e42988. https://doi.org/10.1371/journal.pone.0042988.
5. Tagliabracci VS, Wiley SE, Guo X, Kinch LN, Durrant E, Wen J, et al. A single kinase generates the majority of the secreted phosphoproteome. Cell. 2015;161:1619–32. https://doi.org/10.1016/j.cell.2015.05.028.
6. Nalbant D, Youn H, Nalbant SI, Sharma S, Cobos E, Beale EG, et al. FAM20: an evolutionarily conserved family of secreted proteins expressed in hematopoietic cells. BMC Genomics. 2005;6:11. https://doi.org/10.1186/1471-2164-6-11.
7. Wang X, Hao J, Xie Y, Sun Y, Hernandez B, Yamoah AK, et al. Expression of FAM20C in the osteogenesis and odontogenesis of mouse. J Histochem Cytochem. 2010;58:957–67. https://doi.org/10.1369/jhc.2010.
8. Du EX, Wang XF, Yang WC, Kaback D, Yee SP, et al. Characterization of Fam20C expression in odontogenesis and osteogenesis using transgenic mice. Int J Oral Sci. 2015;7:89–94. https://doi.org/10.1038/ijos.2014.67.
9. Simpson MA, Hsu R, Keir LS, Hao J, Sivapalan G, Ernst LM, et al. Mutations in FAM20C are associated with lethal osteosclerotic bone dysplasia (Raine syndrome), highlighting a crucial molecule in bone development. Am J Hum Genet. 2007;81:906–12. https://doi.org/10.1086/522240.
10. Simpson MA, Scheuerle A, Hurst J, Patton MA, Stewart H, Crosby AH. Mutations in FAM20C also identified in non-lethal osteosclerotic bone dysplasia. Clin Genet. 2009;75:271–6. https://doi.org/10.1111/j.1399-0004.2008.01118.x.
11. Whyte MP, McAlister WH, Fallon MD, Pierpont ME, Bijanki VN, Duan S, et al. Raine syndrome (OMIM #259775), caused by FAM20C mutation, is congenital sclerosing Osteomalacia with cerebral calcification (OMIM 259660). J Bone Min Res. 2017;32:757–69. https://doi.org/10.1002/jbmr.3034.
12. Rejjal A. Raine syndrome. Am J Med Genet. 1998;78:382-5. https://doi.org/10.1002/(sici)1096-8628(19980724)78:4-382::aid-ajmg17-3.0.co;2-e
13. Faundes V, Castillo-Taucher S, Gonzalez-Hormazabal P, Chandler K, Crosby A, Chioza B. Raine syndrome: an overview. Eur J Med Genet. 2014;57:536–42. https://doi.org/10.1016/j.ejmg.2014.07.001.
14. Wang X, Wang S, Li C, Gao T, Liu Y, Rangiani A, et al. Inactivation of a novel FGF23 regulator, FAM20C, leads to hypophosphatemic rickets in mice. PLoS Genet. 2012;8:e1002708. https://doi.org/10.1371/journal.pgen.1002708.
15. Tagliabracci VS, Engel JL, Wiley SE, Xiao J, Gonzalez DJ, Appaiah HN. Dynamic regulation of FGF23 by Fam20C phosphorylation, GalNAc-T3 glycosylation, and furin proteolysis. Proc Natl Acad Sci USA. 2014;111:5520–5. https://doi.org/10.1073/pnas.1402218111.
16. Liu P, Li J, Tang L, Cong W, Jin H, Zhang H, et al. Mutations of family with sequence similarity 20-member C gene causing lethal and nonlethal raine syndrome causes hypophosphatemia rickets. J Cell Physiol. 2023;238:2556–69. https://doi.org/10.1002/jcp.31105.
17. Jani PH, Gibson MP, Liu C, Zhang H, Wang X, Lu Y, Qin C. Transgenic expression of Dspp partially rescued the long bone defects of Dmp1-null mice. Matrix Biol. 2016;52–54:95–112. https://doi.org/10.1016/j.matbio.2015.12.001.
18. Huang B, Sun Y, Maciejewska I, Qin D, Peng T, McIntyre B. Distribution of SIBLING proteins in the organic and inorganic phases of rat dentin and bone. Eur J Oral Sci. 2008;116:104–12. https://doi.org/10.1111/j.1600–0722.2008.00522.x.
19. Sheth J, Bhavsar R, Gandhi A, Sheth F, Pancholi D. A case of Raine syndrome presenting with facial dysmorphy and review of literature. BMC Med Genet. 2018;19:76. https://doi.org/10.1186/s12881-018-0593-x.
20. Mameli C, Zichichi G, Mahmood N, Elalaoui SC, Mirza A, Dharmaraj P. Natural history of non-lethal Raine syndrome during childhood. Orphanet J Rare Dis. 2020;15:93. https://doi.org/10.1186/s13023-020-01373-0.
21. Rafaelsen SH, Raeder H, Fagerheim AK, Knappskog P, Carpenter TO, Johansson S. Exome sequencing reveals FAM20c mutations associated with fibroblast growth factor 23-related hypophosphatemia, dental anomalies, and ectopic calcification. J Bone Min Res. 2013;28:1378–85. https://doi.org/10.1002/jbmr.1850.
22. Takeyari S, Yamamoto T, Kinoshita Y, Fukumoto S, Glorieux FH, Michigami T, et al. Hypophosphatemic osteomalacia and bone sclerosis caused by a novel homozygous mutation of the FAM20C gene in an elderly man with a mild variant of Raine syndrome. Bone. 2014;67:56–62. https://doi.org/10.1016/j.bone.2014.06.026.
23. Marie PJ, Glorieux FH. Bone histomorphometry in asymptomatic adults with hereditary hypophosphatemic vitamin D-resistant osteomalacia. Metab Bone Dis Relat Res. 1982;4:249–53. https://doi.org/10.1016/0221–8747(82)90035-2.
24. Reid IR, Murphy WA, Hardy DC, Teitelbaum SL, Bergfeld MA, Whyte MP. X-linked hypophosphatemia: skeletal mass in adults assessed by histomorphometry, computed tomography, and absorptiometry. Am J Med. 1991;90(91):63–9. https://doi.org/10.1016/0002-9343.
25. Mäkitie O, Pereira RC, Kaitila I, Turan S, Bastepe M, Laine T. Long-term clinical outcome and carrier phenotype in autosomal recessive hypophosphatemia caused by a novel DMP1 mutation. J Bone Min Res. 2010;25:2165–74. https://doi.org/10.1002/jbmr.105.
26. Koike T, Mikami T, Tamura JI, Kitagawa H. Altered sulfation status of FAM20C-dependent chondroitin sulfate is associated with osteosclerotic bone dysplasia. Nat Commun. 2022;13:7952. https://doi.org/10.1038/s41467-022-35687-3.
27. Palma-Lara I, Pérez-Ramírez M, Alonso-Themann PG, Espinosa-García AM, Godinez-Aguilar R, Bonilla-Delgado J. FAM20C overview: classic and novel targets, pathogenic variants and Raine Syndrome Phenotypes. Int J Mol Sci. 2021;22:8039. https://doi.org/10.3390/ijms22158039.
28. Eltan M, Alavanda C, Yavas Abali Z, Ergenekon P, Yalındag Ozturk N, Sakar M, Dagcinar A, Kirkgoz T, Kaygusuz SB, Gokdemir Y, Elcioglu HN, Guran T, Bereket A, Ata P, Turan S. A Rare cause of Hypophosphatemia: Raine Syndrome changing clinical features with age. Calcif Tissue Int. 2020;107:96–103. https://doi.org/10.1007/s00223-020-00694-3.

Publisher's note